An Assessment of the High-gain Streckeisen STS2 Seismometer for Routine Earthquake Monitoring in the United States

By D. E. McNamara, R.P. Buland and H.M. Benz

Open-File Report 2005-1437

U.S. Department of the Interior
U.S. Geological Survey

U.S. Department of the Interior
Gale A. Norton, Secretary

U.S. Geological Survey
P. Patrick Leahy, Acting Director

U.S. Geological Survey, Reston, Virginia 2006

For product and ordering information:
World Wide Web: http://www.usgs.gov/pubprod
Telephone: 1-888-ASK-USGS

For more information on the USGS—the Federal source for science about the Earth, its natural and living resources, natural hazards, and the environment:
World Wide Web: http://www.usgs.gov
Telephone: 1-888-ASK-USGS

Contents

Figures

Tables

An Assessment of the High-gain Streckeisen STS2 Seismometer for Routine Earthquake Monitoring in the United States

By D. E. McNamara, R.P. Buland, and H.M. Benz[1]

Abstract

Objective. In this document, we report the results of a study to determine if the Streckeisen STS2 high-gain seismometer is appropriate for use by the United States Geological Survey's (USGS) Advanced National Seismic System (ANSS) for routine earthquake monitoring in the United States (US).

Issue. At issue is whether the high-gain STS2, with a sensitivity of 20,000 volts/meter/sec, can produce onscale recordings of earthquake activity within the continental US, or whether the low-gain STS2, with a sensitivity of 1500 volts/meter/sec, is more appropriate for earthquake monitoring due to the relatively lower input velocity required for clipping the recording system. The test ANSS backbone station configuration, considered in this study, consists of an STS2 broadband seismometer coupled to a Quanterra Q330 digitizer. The Q330 has a channel sensitivity of 4.19e5 counts/volt and a clip level of 8.38e6 = 8388608 counts (2e23) (20 volts). Therefore, an input ground velocity of only 0.001 m/sec will clip the high-gain system while an input ground velocity of 0.013 m/sec, a factor of 13 larger, is required to clip the lower-gain configuration.

Methods. In this report, we use three different methods to examine the levels of input ground velocity expected during routine earthquake monitoring within the continental US. These methods include:

1. Computing peak ground velocity (PGV) expected at each ANSS backbone station from the USGS's 10 percent probability of exceedance in 30 years 1Hz spectral acceleration maps (fig. 1).
2. Modeling the amplitude of PGV at regional distances using Brune source scaling (fig. 2).
3. Analysis of the September 2004, M6 Parkfield earthquake at four broadband seismic stations within 1000km of the epicenter (figs. 2 and 3).

Recommendation: Based on the analysis of the three methods discussed above, it is our recommendation that the low-gain STS2 is more appropriate for routine earthquake monitoring in the US. Method 1 indicates that if the high-gain configuration is used at all ANSS backbone stations, all can be expected to clip given the ground-shaking levels expected in the next 30 years. Methods 2 and 3 indicate that an M6 will clip stations within approximately 875 km of the epicenter. The high-gain STS2 is more useful for recording teleseismic events on a global scale but not suitable for onscale recording of moderate to large earthquakes within the continental US.

[1] USGS ANSS, Golden, CO

Methods:

I. PGV computed from 1Hz Spectral Acceleration Map.

In this analysis we use the 1 Hz spectral acceleration 10% probability of exceedance in 30 years to calculate the expected PGV at each ANSS backbone station within the continental US (Frankel et al., 2002). The method includes the following procedures:

1. For each ANSS station, determine *%g* from the 1 Hz spectral acceleration map (fig. 1) and convert to *g* (*g = 0.01* %g*) where *1g=980cm/s/s*.
2. Compute PGV in m/sec after (Newmark and Hall, 1982) where *PGV = 594.8 * g / (2*•)*.
3. Compare PGV to clipping velocity of low and high-gain recording systems.

Results from this analysis are summarized in table 1 and in figure 1. All high-gain STS2's will clip the Q330 digitizer given the input PGV computed from the 10 percent probability of exceedance spectral acceleration in the next 30 years. In contrast, 70 percent of the low-gain STS2's will clip in the regions with the highest expected input ground velocity. Stations in the midcontinent are not expected to clip (fig. 1). The high level of clipped stations for the low and high gain STS2 seismometers indicate the importance of colocated low gain accelerometers if onscale recording of all large motion is desired.

II. Brune Source Modeling

In this analysis, we calculate expected shear-wave amplitude using the source scaling models of Brune (1970) and Brune (1971) for a range of distances (25-1200 km) and magnitudes (M5-7). We then compare the modeled amplitude to the velocity required to clip the high and low gain recording systems. (fig. 2). The method includes the following procedures.

1. For each Mw, determine Mo from: Mw = 0.667 log(Mo) – 10.7 (*Kanimori,* 1977).

2. For each Mo, determine fault dimension from: Mo = $2.29\sigma r^3$ dyne-cm (*Brune* 1970, 1971) where $\sigma = 1.0*10^8$ effective stress.

3. For each fault dimension, determine source corner frequency from:

$$r = \frac{2.21\beta}{2\pi fc}$$ fault dimension in cm *(Brune* 1970, 1971*)*.

where β = shear wave velocity = 3.5km/s
fc = source corner frequency

4. Find angular frequency (*fm*), by bisection, where Brune source spectrum is a maximum given ANSS short-period detection filters (0.5-12 Hz).

5. For each source-receiver distance (from 25-1100 km), calculate Shear-wave PGV amplitude (*As*) in m/sec from:

$$As = \frac{Mo}{4\mu\beta} \bullet \frac{fmfc^2}{fm^2} + \frac{fc^2}{\Delta} \qquad \textit{(Brune 1970, 1971)}.$$

where μ = rigidity,
fc = source corner frequency,
fm = effective frequency where amplitude is maximum,
β = shear-wave velocity (3.5km/s), and
• = source-receiver distance.

5. Apply attenuation to Shear-wave amplitude (As).

$$As = \frac{As}{\Delta^{\gamma}} \bullet e^{\frac{-\pi fm\Delta}{Q\beta}}$$

where γ = geometric spreading (0.5)
Q = Quality factor.
Northern California (Erickson et al. 2004).
$Q = 105fm^{0.67}$

6. Multiply the modeled amplitude by the total sensitivity of the high-gain recording system (8.38e9 counts/m/s) and plot corrected PGV as a function of epicentral distance.

Results from this analysis are shown in figure 2 along with the input clipping velocities for the high and low-gain systems. From figure 2, we see that an earthquake with a magnitude of 6.0 will clip the high-gain system at distances less than about 875 km while the low-gain system will clip at distances less than 150 km. A magnitude 5.0 will clip the high-gain system at distances less than 175 km.

III. M6.0 Parkfield Earthquake, September 2004

To verify the amplitude modeling results calculated in Method II we analyzed the amplitudes of the September 2004, M6 Parkfield earthquake at four broadband seismic stations within 1100 km of the epicenter. Four stations that cooperate with the ANSS from the US, BRK and IU networks were used in the analysis. In each case, the M6.0 Parkfield earthquake did not clip any of the broadband stations. The stations used in the analysis include:

HOPS: Hopland, Mendicino County California. BRK network.
Digitizer: Quanterra Q380 recording at 20 samples/second.
seismometer : STS1.

COR: Corvallis Oregon, US/IU network.
Digitizer: Quanterra Q380 recording at 20 samples/second.
Seismometer: STS1(sens 2.51e3 counts/volt)

WDC: Whiskeytown Dam, California, US/BRK network.
Digitizer: Quanterra Q380 recordinga t 20 samples/second.
Seismometer: Low-gain STS2 (sens 1500 counts/volt).

MOD: Modoc County California, BRK network.
Digitizer: Quanterra QX-80 recording at 20 samples/second.
Seismometer: STS1 (sens 2240 counts/volt).

The individual station instrument responses (Appendix 1) were deconvolved from the data and converted to displacement. We then convolved the data from each station with total response of the Q330 and high-gain STS2 (Appendix 1). For each station, peak amplitude (PGV) was measured from the largest arrivals on the vertical component of motion (BHZ), which at regional distances is dominated the multiply reflected crustal shear-wave, *Lg*. PGV is then plotted as a function of epicentral distance (fig. 2) (Table 2).

From figure 2, it is apparent that the three stations closest to the Parkfield earthquake (HOPS, WDC, MOD) would have clipped if the high-gain recording systems were in use. In contrast, the stations did not actually clip with their current instrumentation and would not have clipped if the low-gain STS2 were deployed (fig. 2). Station COR, at 1003 km, would not have clipped either the low or high-gain system. Figure 3 shows the amplitude of the Parkfield M6.0 recorded at MOD at 667 km for three different instrumentation configurations. MOD currently has an STS1 (black line, fig. 3) and did not clip on the Parkfield earthquake. Figure 3 also demonstrates that a high-gain STS2 recording system would have been clipped by the Parkfield earthquake at MOD at a distance of 667 km.

Conclusions

Based on the results from this analysis, it is apparent that the high-gain STS2 is not optimal for routine earthquake monitoring in the US. The gain level is sufficiently high that moderate size (M6.0) earthquakes would clip the Quanterra Q330 digitizer at distances less than 875 km. This is unacceptable if we hope to record these events onscale. Instead, the high-gain STS2 is more appropriate for remote seismic stations where weaker ground motion is expected.

References Cited

Brune, J., 1970, Tectonic stress and the spectra of seismic shear waves from earthquakes, J. Geophys. Res., 75, 4997-5009.

Brune, J., 1971, Correction, J. Geophys. Res., 76, 5002.

Erickson, D., D. McNamara, H. Benz, 2004, Frequency-dependent Lg Q within the Continental United States, *Seism. Soc. Am. Bull*, 94, 1630-1643.

Frankel, A., Petersen, M., Mueller, C., Haller, K., Wheeler, R., Leyendecker, E., Wesson, R., Harmsen, S., Cramer, C., Perkins, D., and Rukstales, K., 2002, Documentation for the 2002 update of the national seismic hazard maps, U.S. Geological Survey Open-File Report 02-420, 39 pages.

Kanimori, 1977, The energy release in great earthquakes, J. Geophys. Res, 82, 2881-2987.

Newmark, N.M. and Hall, W.J., 1982, "Earthquake Spectra and Design" EERI monograph.

Table 1. Percent Clip for standard and high-gain STS2 from Method I.

Sta	latitude	longitude	%g	g	PGV (m/s)	SG %clip	HG %clip
AAM	42.300999	-83.656998	1.330970	0.013310	0.0125997	0.944757	12.6018
ACSO	40.231998	-82.983002	1.736430	0.017364	0.016438	1.23256	16.4407
AHID	42.764999	-111.099998	13.802000	0.138020	0.130657	9.79702	130.679
ANMO	34.945999	-106.457001	4.496410	0.044964	0.0425654	3.19167	42.5725
BINY	42.199001	-75.986000	1.559670	0.015597	0.0147647	1.10709	14.7671
BLA	37.210999	-80.420998	2.192460	0.021925	0.020755	1.55626	20.7584
BLO	39.172001	-86.522003	2.566570	0.025666	0.0242965	1.82182	24.3006
BMN	40.431000	-117.222000	8.432590	0.084326	0.0798274	5.98567	79.8407
BOZ	45.599998	-111.633003	9.916620	0.099166	0.093876	7.03907	93.8916
BW06	42.778000	-109.556000	4.586710	0.045867	0.0434202	3.25577	43.4275
CBKS	38.813999	-99.737000	1.145350	0.011454	0.0108425	0.812999	10.8443
CBN	38.205002	-77.373001	1.408630	0.014086	0.0133349	0.999882	13.3371
CCM	38.056000	-91.245003	3.163960	0.031640	0.0299517	2.24586	29.9567
CMB	38.035000	-120.385002	9.530080	0.095301	0.0902169	6.7647	90.2318
COR	44.585999	-123.303001	9.505110	0.095051	0.0899805	6.74697	89.9954
DAC	36.277000	-117.594002	16.641701	0.166417	0.157539	11.8127	157.565
DUG	40.195999	-112.816002	5.698430	0.056984	0.0539444	4.04489	53.9533
DWPF	28.110001	-81.432999	0.653747	0.006537	0.00618872	0.464047	6.18975
ELK	40.744999	-115.238998	4.964200	0.049642	0.0469938	3.52372	47.0016
EYMN	47.945999	-91.495003	0.310897	0.003109	0.00294312	0.220683	2.94361
GOGA	33.410999	-83.467003	2.422660	0.024227	0.0229342	1.71967	22.938
HAWA	46.393002	-119.532997	5.147710	0.051477	0.048731	3.65398	48.7391
HKT	29.950001	-95.833000	0.816093	0.008161	0.00772557	0.579284	7.72685
HLID	43.561001	-114.418999	5.659060	0.056591	0.0535717	4.01695	53.5806
HOPS	38.993999	-123.071999	36.925400	0.369254	0.349556	26.2106	349.614
HRV	42.506001	-71.557999	1.748700	0.017487	0.0165541	1.24127	16.5569
HWUT	41.606998	-111.565002	9.699410	0.096994	0.0918198	6.88489	91.835
ISCO	39.799999	-105.612999	1.654140	0.016541	0.015659	1.17415	15.6616
JCT	30.479000	-99.802002	0.503462	0.005035	0.00476604	0.35737	4.76683
JFWS	42.914001	-90.248001	1.112710	0.011127	0.0105335	0.78983	10.5353
KNB	37.016998	-112.821999	4.696350	0.046964	0.0444582	3.33359	44.4655

Sta	latitude	longitude	%g	g	PGV	SG %clip	HG %clip
LBNH	44.240002	-71.926003	2.280530	0.022805	0.0215887	1.61878	21.5923
LKWY	44.564999	-110.400002	12.156100	0.121561	0.115076	8.62871	115.095
LRAL	33.035000	-86.998001	2.224120	0.022241	0.0210547	1.57874	21.0582
LSCT	41.678001	-73.223999	1.604300	0.016043	0.0151872	1.13877	15.1897
LTX	29.334000	-103.667000	2.222410	0.022224	0.0210385	1.57752	21.042
MCWV	39.658001	-79.846001	1.584410	0.015844	0.0149989	1.12465	15.0014
MIAR	34.546001	-93.572998	2.096850	0.020968	0.0198499	1.4884	19.8532
MNV	38.432999	-118.153000	17.172800	0.171728	0.162567	12.1897	162.594
MOD	41.903000	-120.306000	8.412420	0.084124	0.0796365	5.97135	79.6497
MVU	38.505001	-112.210999	7.899620	0.078996	0.074782	5.60736	74.7944
MYNC	35.074001	-84.127998	3.033970	0.030340	0.0287212	2.15359	28.726
NCB	43.971001	-74.223999	2.356310	0.023563	0.0223061	1.67257	22.3098
NEW	48.263000	-117.120003	3.619540	0.036195	0.0342645	2.56924	34.2702
NHSC	33.106998	-80.178001	3.245180	0.032452	0.0307206	2.30351	30.7257
OCWA	47.749001	-124.178001	16.503599	0.165036	0.156232	11.7147	156.258
OXF	34.512001	-89.408997	3.180920	0.031809	0.0301123	2.2579	30.1173
PAS	34.147999	-118.171997	37.812199	0.378122	0.357951	26.8401	358.01
PFO	33.609001	-116.455002	33.764099	0.337641	0.319629	23.9666	319.682
PLAL	34.981998	-88.075996	3.189070	0.031891	0.0301894	2.26368	30.1945
RSSD	44.119999	-104.036003	1.247570	0.012476	0.0118102	0.885558	11.8121
SAO	36.764999	-121.445000	43.401501	0.434015	0.410862	30.8075	410.93
SDCO	37.745998	-105.500999	2.562140	0.025621	0.0242546	1.81867	24.2586
SLM	38.636002	-90.236000	3.590330	0.035903	0.033988	2.54851	33.9936
SSPA	40.636002	-77.888000	1.393160	0.013932	0.0131884	0.988901	13.1906
TPH	38.075001	-117.223000	9.866430	0.098664	0.0934009	7.00345	93.4164
TPNV	36.948002	-116.249001	8.793650	0.087936	0.0832454	6.24196	83.2592
TUC	32.310001	-110.783997	2.316950	0.023170	0.0219335	1.64463	21.9371
WCI	38.229000	-86.293999	2.863830	0.028638	0.0271106	2.03282	27.115
WDC	40.580002	-122.540001	12.858200	0.128582	0.121723	9.12708	121.743
WMOK	34.737999	-98.780998	1.342820	0.013428	0.0127119	0.953168	12.714
WUAZ	35.516998	-111.374001	3.457260	0.034573	0.0327283	2.45405	32.7337
WVOR	42.433998	-118.637001	4.970230	0.049702	0.0470509	3.528	47.0587
WVT	36.130001	-87.830002	3.815320	0.038153	0.0361179	2.70821	36.1239
EGMT	47.950001	-109.779999	1.126660	0.011267	0.0106656	0.799733	10.6673
DGMT	48.580002	-104.199997	0.691208	0.006912	0.00654335	0.490638	6.54444

Sta	latitude	longitude	%g	g	PGV	SG %clip	HG %clip
VKMN	48.220001	-96.410004	0.356017	0.003560	0.00337025	0.25271	3.37081
COWI	46.060001	-89.260002	0.589685	0.005897	0.00558227	0.418573	5.5832
GRMI	44.660000	-84.720001	0.939180	0.009392	0.00889078	0.666654	8.89226
OGNE	41.130001	-101.720001	1.013730	0.010137	0.00959651	0.719572	9.5981
SCIA	42.020000	-93.160004	1.104300	0.011043	0.0104539	0.783861	10.4556
PDNY	44.669998	-74.980003	2.698170	0.026982	0.0255423	1.91523	25.5466
MIME	45.660000	-68.709999	2.144410	0.021444	0.0203001	1.52216	20.3035
MONC	35.200001	-78.070000	1.583770	0.015838	0.0149928	1.1242	14.9953
ATAL	31.020000	-87.489998	1.479430	0.014794	0.0140051	1.05014	14.0074
GHTX	27.170000	-98.120003	0.288432	0.002884	0.00273045	0.204736	2.7309
SNSD	45.060001	-99.510002	0.750744	0.007507	0.00710694	0.532897	7.10812
ANND	47.880001	-100.239998	0.509268	0.005093	0.004821	0.361491	4.8218
AMTX	35.180000	-101.870003	0.955765	0.009558	0.00904778	0.678426	9.04928
BNMN	46.360001	-94.199997	0.442334	0.004423	0.00418737	0.31398	4.18806
BRMT	45.299999	-108.910004	3.247320	0.032473	0.0307409	2.30503	30.746
KCCO	38.759998	-102.790001	1.054920	0.010549	0.00998644	0.74881	9.9881
ERPA	42.130001	-80.089996	1.453010	0.014530	0.013755	1.03138	13.7573
SEKY	36.599998	-83.720001	2.942140	0.029421	0.0278519	2.08841	27.8565
CLKS	37.029999	-97.610001	1.406600	0.014066	0.0133156	0.998441	13.3178
NNNM	36.889999	-109.690002	1.343560	0.013436	0.0127189	0.953694	12.721
MNTX	31.697001	-105.382004	2.613080	0.026131	0.0247368	1.85483	24.7409

Table 2. Parkfield PGV amplitude convolved with high-gain system response.

Sta	latitude	longitude	distance (km)	PGV (m/s)
MOD	41.9033	-120.305	667	0.00183
HOPS	38.9939	-123.071	421	0.00305
WDC	40.5800	-122.539	558	0.00190
COR	44.5857	-123.303	1003	0.00080

Appendix 1: Instrument responses

High-gain STS2 and Q330:
ZEROS 3
0. 0.
0. 0.
0. 0.
POLES 5
-3.70237E-02 3.70244E-02
-3.70237E-02 -3.70244E-02
-251.327 0.
-118.634 423.065
-118.634 -423.065
CONSTANT 4.05950E+17

HOPS:
ZEROS 3
0. 0.
0. 0.
0. 0.
POLES 4
-1.23400E-02 1.23400E-02
-1.23400E-02 -1.23400E-02
-39.1800 49.1200
-39.1800 -49.1200
CONSTANT 3.88355E+12

WDC:
ZEROS 3
0. 0.
0. 0.
0. 0.
POLES 5
-3.70237E-02 3.70244E-02
-3.70237E-02 -3.70244E-02
-251.327 0.
-118.634 423.065
-118.634 -423.065
CONSTANT 2.92868E+16

MOD:
ZEROS 3
0. 0.
0. 0.
0. 0.
POLES 4
-1.23400E-02 1.23400E-02
-1.23400E-02 -1.23400E-02

```
  -19.5900    24.5600
  -19.5900   -24.5600
CONSTANT     9.85368E+11

COR:
ZEROS   3
 0.  0.
 0.  0.
 0.  0.
POLES   4
  -1.23400E-02    1.23400E-02
  -1.23400E-02   -1.23400E-02
  -39.1800    49.1200
  -39.1800   -49.1200
CONSTANT     4.18246E+12
```

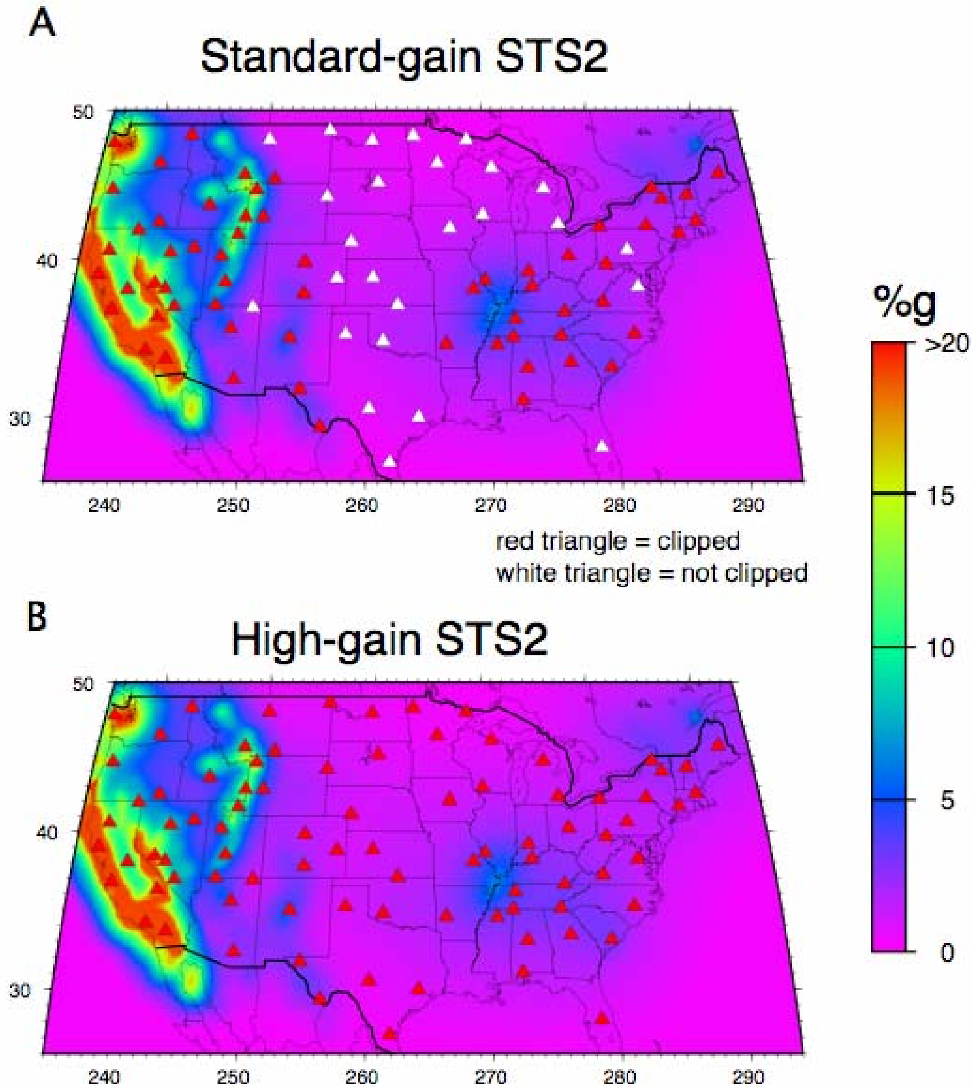

Figure 1: 10 percent in 30 years 1 Hz spectral acceleration for the United States.

A) Assuming Low-gain STS2 instrumentation (red triangles = clipped stations).

B) Assuming high-gain STS2 instrumentation (red triangles = clipped stations).

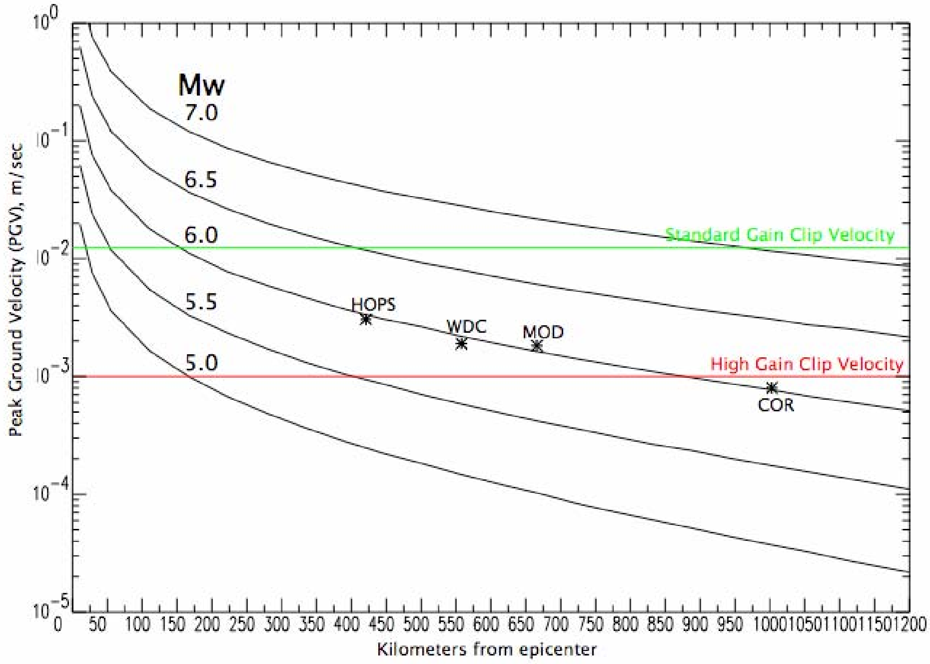

Figure 2: Brune source modeled PGV as a function of epicentral distance. Also plotted is the PGV measured at four stations from the September 2004 Parkfield M6.0 earthquake.

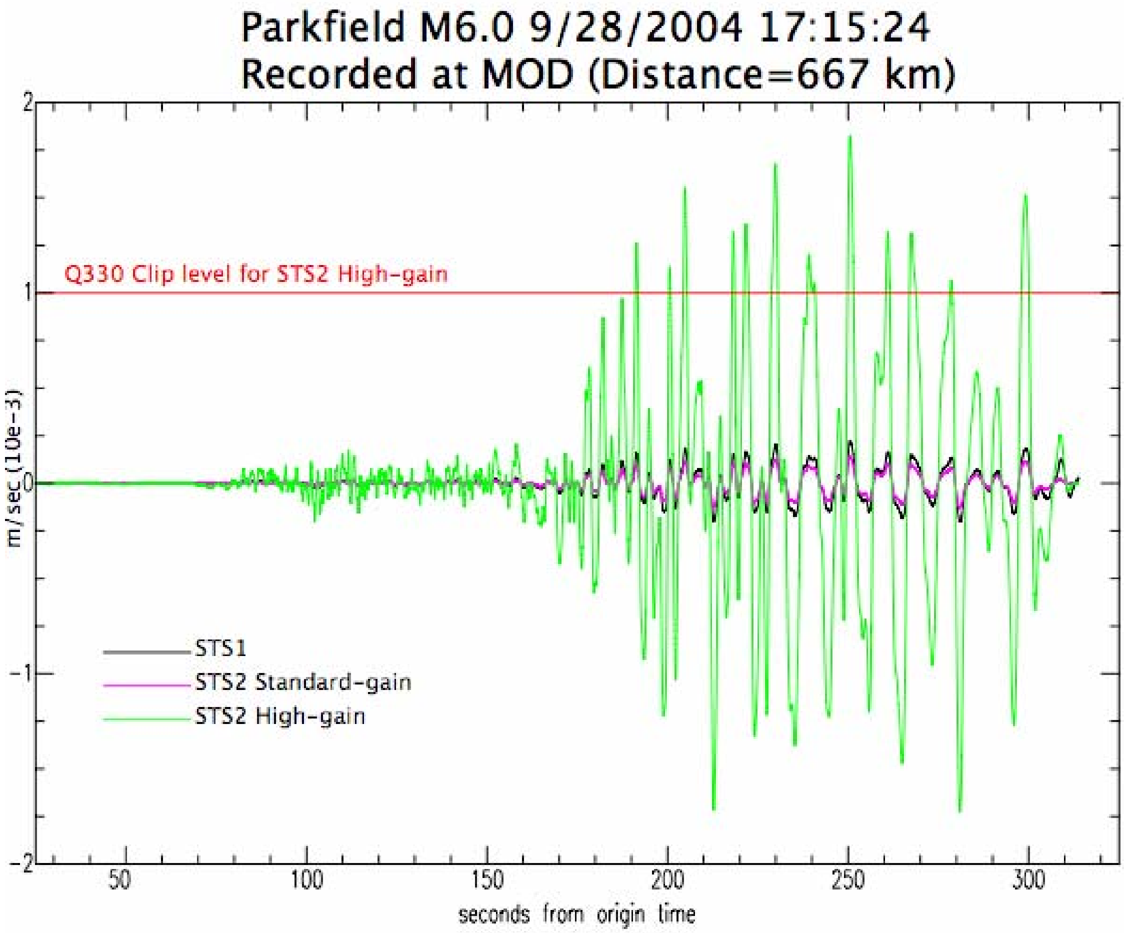

Figure 3: Seismogram of the Parkfield M6.0 recorded at MOD. Black line is the original seismogram using an STS1 seismometer. Magenta line is the waveform convolved with the low-gain recording system. Green line is the waveform convolved with the high-gain system.